Elliptical Orbits of Microspheres in an Evanescent Field

Lulu Liu,[1] Simon Kheifets,[1] Vincent Ginis,[1,2] Andrea Di Donato,[1,3] and Federico Capasso[1,*]

[1] *Harvard University, 29 Oxford Street, Cambridge, MA 02138*
[2] *Vrije Universiteit Brussel, Pleinlaan 2, 1050 Brussel, Belgium*
[3] *Università Politecnica delle Marche, Via Brecce Bianche 60131, Ancona, Italy*

We examine the motion of periodically driven, optically tweezed microspheres in fluid and find a rich variety of dynamic regimes. We demonstrate, in experiment and in theory, that mean particle motion in 2D is rarely parallel to the direction of the applied force, and can even exhibit elliptical orbits with non-zero orbital angular momentum. The behavior is unique in that it depends neither on the nature of the microparticles nor that of the excitation; rather, angular momentum is introduced by the particle's interaction with the anisotropic fluid and optical trap environment. We find overall this motion to be highly tunable and predictable.

Introduction. Recently, much work has gone into the investigation of optical forces on micro- and nanoparticles near surfaces, primarily in the context of an electric field localized by a micro-structured surface [1–5]. Surface-based geometries have raised theoretical excitement due to, for instance, their ability to significantly enhance optical forces [6–8], as well as the emergence of lateral forces due to the extraordinary momentum and spin in evanescent waves [9–12]. From an applied point of view, such geometries can enable miniaturization and parallelization of efficient optical traps enabling integration into optofluidic devices [13, 14]. Moreover, light-controlled microspheres near surfaces have found applications as force transducers [15–18], pumps and switches [19, 20], and in general their collective manipulation is an advancing field [21–23].

However, in the case where a microparticle is within several diameters of a surface, optical and hydrodynamic surface effects cannot be neglected. Effects arising from optical coupling or reflections can complicate trapping and detection schemes [24], and hydrodynamic interactions can cause the motion of a microparticle to become highly nontrivial [25]. Despite this, little quantitative study has been done on the dynamics of optically driven particles near a surface. In studies introducing new schemes to optically manipulate matter, the particle's response function is often ignored [11, 12, 26–29].

In this work, we investigate the dynamics of a system with both near field optical forces and surface-induced hydrodynamic effects (see Fig. 1). By driving the particle with an oscillating force from a modulated evanescent field and tracking the particle's motion closely in two dimensions, we map out a range of dynamics which can arise from the interplay of optical and hydrodynamic surface effects. We find that the magnitude and direction of the force depends on particle size. We also observe that the trajectory of the particle does not simply follow the direction of the force, but that its shape and orientation varies with modulation frequency and distance from the surface, a result of the anisotropy in both the hydrodynamic drag and the optical trap spring constant.

In particular, we discover that elliptical motion of an optically trapped microbead can be achieved without the use of nanofabrication or specially tailored beams carrying orbital angular momentum. The measured mean intrinsic angular momentum of these trajectories agrees with linear theory predictions and is within an order of magnitude of what has been thus far reported in studies using structured light [30, 31].

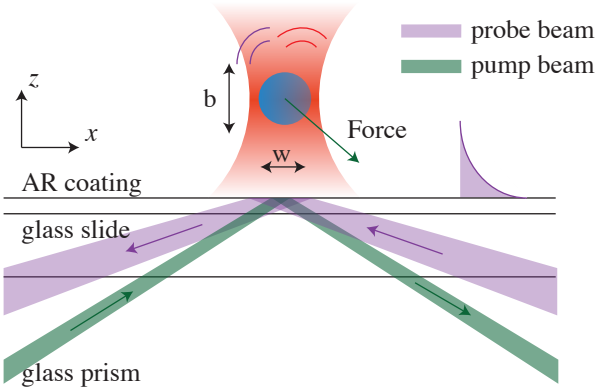

FIG. 1: The optically trapped microsphere in its anisotropic environment. The optical trap (660 nm) has a Rayleigh length, b, larger than the beam waist, w, resulting in a restoring force approximately five times stronger in the lateral direction. Additionally, near-wall hydrodynamic coupling results in anisotropic drag which is consistently larger in the vertical direction. As a result, the particle has a different response function in the two directions. The optical force of the pump beam has components in z and x. At a driving frequency between the two cut-off frequencies, the particle's response can have large phase differences between the two directions, generating elliptical orbits. For a detailed description of the setup, see Fig. S1.

Forces on a driven, trapped microsphere An optically trapped microsphere in fluid is well-modeled as a stochastically driven, damped harmonic oscillator in three dimensions [32, 33]:

$$m^\star \ddot{x}_i(t) = -\kappa_{ij} x_j(t) - \gamma_{ij} \dot{x}_j(t) + B_i(t) + F_i(t). \quad (1)$$

The terms on the right of Eq. (1) correspond, in order, to the restoring force of the optical trap, the dissipative drag in fluid, the stochastic force due to thermal fluctuations, and an externally applied force. Here, we apply a force

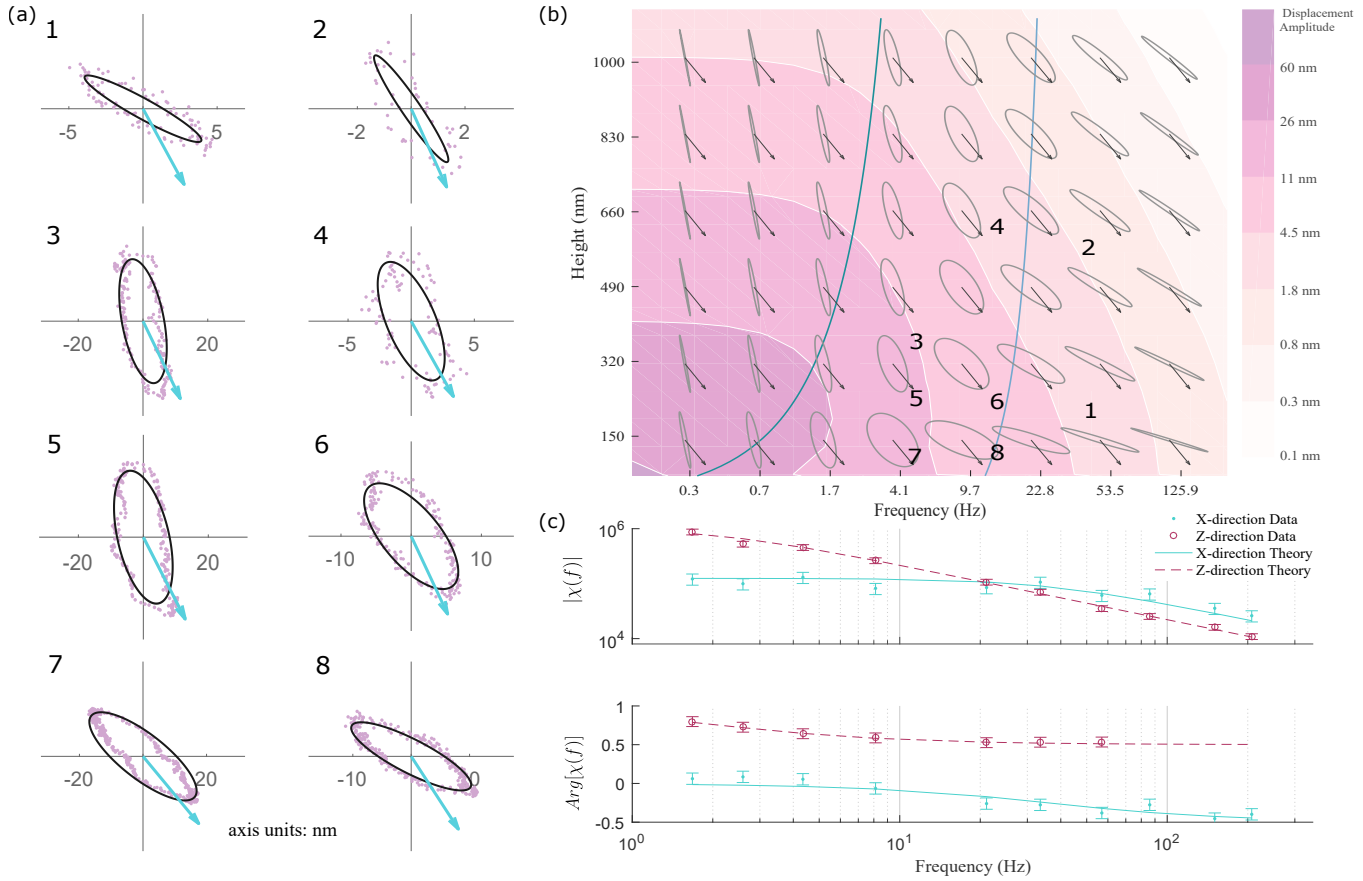

FIG. 2: (a) Predicted and measured 2D motion of a 1 μm radius bead when driven by a periodic optical force from an evanescent field. The blue arrows indicate the direction of the optical force. Each tile in (a) corresponds to a particular height (z) and modulation frequency (ω_0), and are numbered corresponding to their location on the grid (b). The details of the measurement parameters are given in the Suppl. Mat. (b) Grid of predicted particle trajectories where the horizontal axis represents the driving frequency, and the vertical axis is the height above the surface. The displacement amplitude in nanometers is defined as the length of the semi-major axis of each orbit. Calculated cutoff frequencies in the x and z directions are drawn as blue lines. At all heights, the cutoff frequency in the z direction is lower than that in the x direction, due to a larger trap stiffness in the lateral direction. (c) Measured amplitude and phase of frequency-dependent mechanical susceptibility, $\chi(f)$, at a height of 400 nm, compared with predictions.

and consider motion only in the two measured (x and z) dimensions.

Due to the symmetries in our system, the trap stiffness, κ_{ij} is a diagonal tensor. For a single beam optical trap, its diagonal elements are not equal, $\kappa_x \neq \kappa_z$, that is, the harmonic potential is anisotropic. Usually, magnitude of the spring constant in the lateral direction is several times that of the axial one [34]. In our model describing the particle motion, we approximate that κ_i is a constant in z, an assumption that is generally valid until the separation becomes smaller than the Debye length in water [35].

In the absence of boundary effects, viscous drag, γ, is isotropic, given by Stokes' Law, $\gamma_0 = 6\pi\eta R$, where η is the viscosity of the fluid and R is the radius of a sphere. The presence of the boundary results in an anisotropic, height-dependent drag coefficient[36, 37]. The predicted drag in the direction perpendicular to the surface (z) is always larger than that in the lateral direction (x) [35]. Due to the spherical symmetry of the particle, in low Reynolds number hydrodynamics (Re $\ll 1$), we may assume that the drag forces parallel and perpendicular to a plane boundary are uncoupled, such that γ_{ij} is diagonal with unequal elements [38].

$\vec{B}(t)$ is the fluctuating thermal force due to collisions between the microparticle and molecules of the fluid. In each dimension, the fluctuations are expected to be uncorrelated, with $\langle B_i(t)\rangle = 0$, where $\tilde{B}(\omega)$ is spectrally flat. Its mean-squared magnitude is predicted by the fluctuation-dissipation theorem to be $\langle B_i(t)^2\rangle = 2\gamma_i k_B T$, where k_B is the Boltzmann constant. It's important to note that thermal noise increases not only with temperature but also with increased viscous drag and is the dominant source of noise in our system [18].

Lastly, the external force, which drives the periodic motion of the particle, is an optical force produced by the interaction of the microsphere with the evanescent field of a totally internally reflected TM-polarized plane wave. In

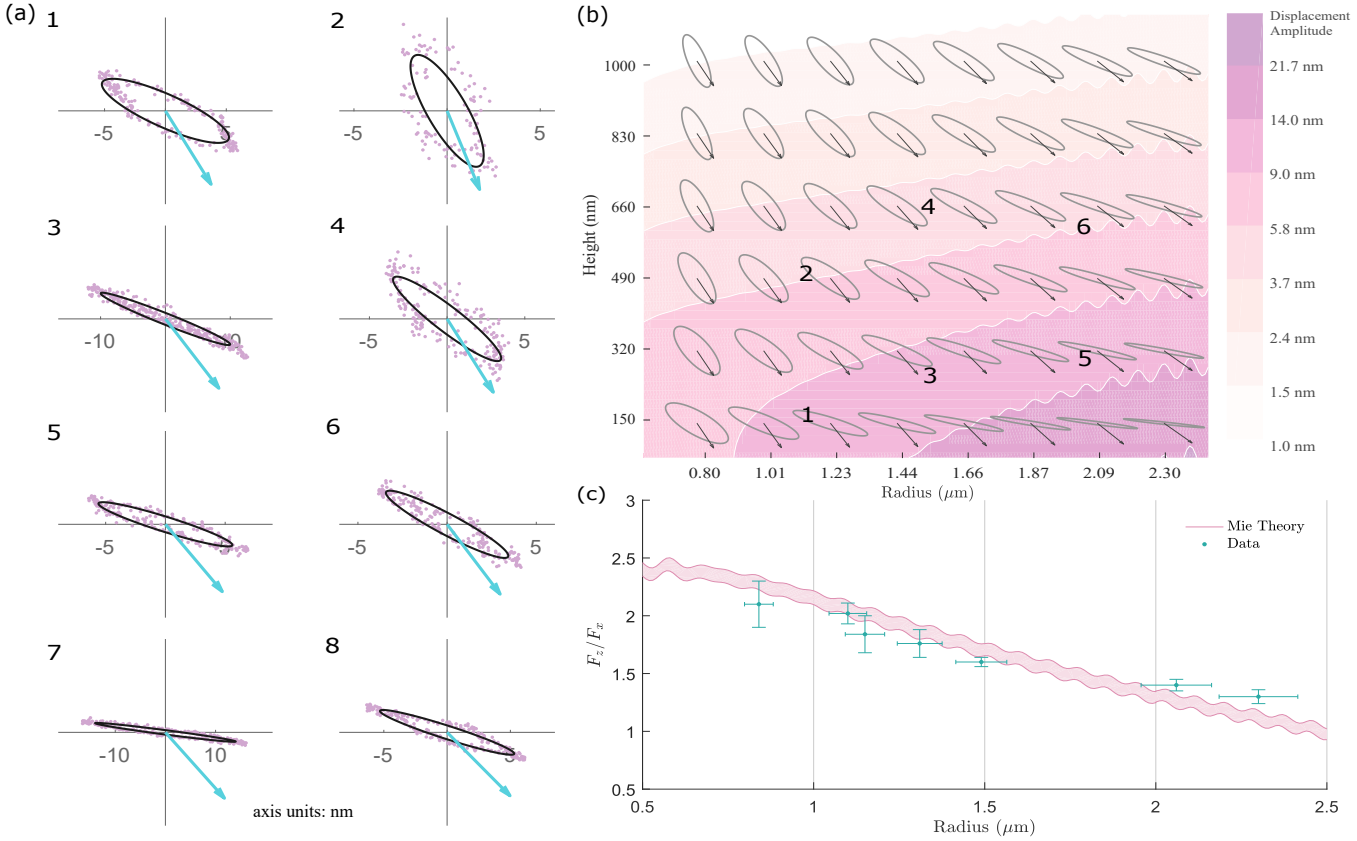

FIG. 3: (a) Predicted and measured motion of 0.6-2.5 μm radius beads when driven by a periodic optical force from an evanescent field that is switched on and off at 20 Hz. The blue arrows indicate the direction of the optical force. Each tile in (a) corresponds to a particular height and bead radius, and are numbered corresponding to their location on the grid (b). The details of the measurement parameters are given in the Suppl. Mat. (b) Grid of predicted particle trajectories based on Mie theory calculations, where the horizontal axis represents bead radius and the vertical axis is the height above the surface. The displacement amplitude in nanometers is defined as the length of the semi-major axis of each orbit. The trajectories labeled 7 and 8 are for a 2.85 μm radius bead, outside the scope of our Mie theory calculations. (c) Ratio of measured optical forces in the z and x directions compared with Mie theory. Shaded area shows the uncertainty in the microsphere index of refraction (n=1.575±0.005). Generally, as microparticle radius increases, the direction of the optical force rotates towards the horizontal.

the dipolar approximation, the interaction can be broadly understood to have two components: one proportional to the gradient of the field, which attracts the particle towards the surface, the other proportional to the linear momentum of the wave, which pushes the particle along the surface [35]. For small, lossless particles ($\mathrm{Im}[\alpha] \ll \mathrm{Re}[\alpha]$), the optical force is predominantly oriented along the z direction. But as the particle increases in size, its interaction with the evanescent wave becomes more complex [39]. In this regime, called the Mie regime, light is scattered into every direction in the xz plane. As a result, the direction of the net applied force is observed to rotate towards the horizontal direction. A detailed analysis of the forces acting on the particle in the Mie regime is shown in the Suppl. Mat. [35].

Microparticle mechanical response The mechanical response of our microsphere to an applied force is frequency-dependent and can be found by solving Eq. (1). We can neglect the particle's inertia while working at time scales much larger than the momentum relaxation time, $\tau_p = m^\star/\gamma$, which, in our system, is below 1 μs [40, 41]. Inserting a time-harmonic solution, we then find that

$$\tilde{x}_i(\omega) = \chi_{ij}(\omega)\tilde{F}_j(\omega), \tag{2}$$

in which we identified the mechanical susceptibility $\chi_{ij}(\omega)$ of the system as $(\chi^{-1}(\omega))_{ij} = \kappa_{ij} + i\omega\gamma_{ij}$.

The motion is separable, with two different cutoff frequencies, $f_c = \kappa/2\pi\gamma$, in the x and z directions. Eq. 2 implies that though $F_x(t)$ and $F_z(t)$ may be in phase, as is the case with our optically driven system, $x(t)$ and $z(t)$ need not. The maximum phase lag between motion in the two directions is $\pi/2$, making possible elliptical trajectories of the particle. Furthermore, the linearity of the system ensures that Eq. 2 applies whether the force is random or periodic. Thus, in our case, where the external force on our particle is composed of both a driven and a stochastic component, the thermal motion of the microsphere may be considered separately from the time evolution of the particle's mean position.

Experiment. A schematic of the experiment is shown in Fig. 1 (also see Fig. S1 for details). All experiments are performed at room temperature in a water-filled, closed, 25 μm deep microfluidic chamber. An anti-reflection (AR) coating is applied to the bottom glass-water interface of the chamber to eliminate standing-wave modulation of the trap laser beam [42]. Each polystyrene microsphere is optically trapped by an expanded 660 nm beam from a CW laser focused through a high numerical aperture (NA=1.2) water-immersion objective. The vertical position of the focus, and consequently the height of the trapped bead, is adjusted using a piezo—by lifting and lowering the objective relative to the chamber. In addition to the trap beam, which enters the chamber from above, two lasers, both p-polarized, are incident from below at greater than critical angle (θ_c=61.4°): a low power (<1mW), 637 nm beam acts as the probe for the vertical (z) position of the particle [15, 43] and a second laser (785 nm, around 100 mW power) generates the periodic optical forces which pull on the microparticle. The second beam, which we refer to as the pump beam, is on/off modulated by a chopper set to a desired frequency. A detailed explanation of the analysis may be found in the Suppl. Mat. [35].

Results Fig. 2 plots the predicted and observed 2D trajectories of a 2 μm PS microsphere under the influence of a periodic optical force. Predictions were made based on the optical force, mean trap stiffnesses, and bead radius fitted to experimental data. The measured trajectories are mean trajectories, extracted from 100 s measurements where each point is the averaged 2D position of the particle at a certain phase in the chopper actuation cycle. As the frequency of the modulation is increased, several distinct behaviors are observed which can be understood in relation to the cutoff frequencies in the two spatial directions. Below both cutoff frequencies, the position of the particle is in phase with the applied force. In this case, the particle's motion in x and z are in phase with one another and it undergoes linear oscillations with a direction determined primarily by the ratio of the trap stiffnesses κ_x/κ_z. In our case, the ratio is about 5. Above both cutoff frequencies, the motion is again linear as the oscillations are now out of phase with the applied force in both directions. However, the direction of motion is now determined by the ratio of the damping coefficients γ_x/γ_z. As the particle nears the surface, γ_z diverges while γ_x approaches a constant value, and the motion becomes more and more parallel to the wall. But between the two cutoff frequencies, the motions in the two spatial directions go out of phase with one another and stable, elliptical orbits are established.

In Fig. 3 we compare our measurements against Mie theory predictions for a fixed modulation frequency. As the microparticle radius increases, the net optical force from the evanescent field increases for a given field strength and configuration, and the direction of the force rotates slowly towards the horizontal. In addition, since hindered diffusion theory predicts drag near a surface to increase as a function of the ratio z/R, where z is the separation and R is the radius, increasing radius has similar effects as decreasing separation. Therefore, large beads tend to move parallel to the surface, regardless of their direction of excitation.

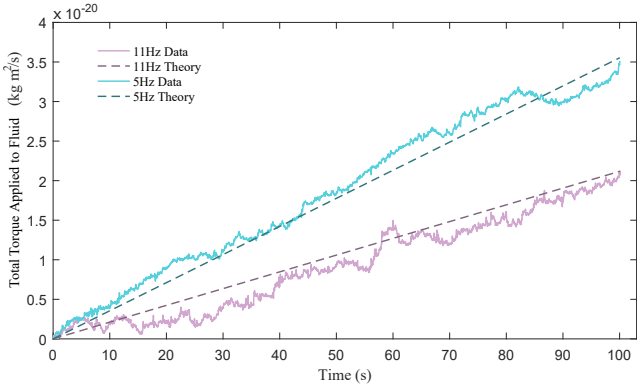

FIG. 4: Measured and predicted torque applied to fluid integrated over time for a 2μm PS bead driven at 11 Hz and 5 Hz frequency at a height of about 200 nm, corresponding to points [5] and [6] in Fig. 2. The force on the bead is the same in both curves.

One manner of quantifying angular motion is to consider the torque applied by the particle to the fluid, $\tau_{app}(t) = \vec{r}(t) \times \gamma\vec{v}(t)$, where γ is the tensor described in Eq. 1. For a particle undergoing steady-state, elliptical motion in fluid, this quantity is on average the same as the torque applied to the particle. Fig. 4 shows τ_{app} accumulating over 100 s for a bead driven at two different frequencies, which agree well with predictions. Another method of quantifying this angular motion is to calculate the constant, non-zero intrinsic orbital angular momentum in the steady state, given by, $\langle L_{in}\rangle = \omega|\tilde{x}||\tilde{z}|\sin(\phi_z - \phi_x)$, where ϕ_x and ϕ_z are the phases of the complex mechanical susceptibilities χ_x and χ_z in the x and z directions, respectively, and $\langle L_{in}\rangle$ is normalized by mass [35]. This quantity is useful in allowing direct comparison with existing reports in literature, where we do not have access to values of the damping parameter, γ, but can estimate velocity and orbital radius. In our unoptimized set-up, the largest L_{in} was measured to be $4.9\times10^{-15}m^2/s$, where $\phi_z - \phi_x$ was closest to $\pi/2$. The configuration for this measurement was a 2 μm diameter bead driven at 4.6 Hz at a separation of around 200 nm from the surface (corresponding to point [5] in Fig. 2). In comparing this value with previous reports for dielectric particles driven by structured light, such as by optical vortices [30, 31], we find our value comparable when normalized by laser power. With optimization of driving frequency and bead radius, or changes in the power or wavelength of the pump beam, further gains may be expected. For details, see Suppl. Mat. [35].

Conclusion Using a highly sensitive detection scheme, we investigated the dynamics of trapped microspheres under the influence of a periodic force. We find good agreement between our model and the measured motion and demonstrate a novel method of generating elliptical orbits with sustained, non-zero orbital angular momentum.

We acknowledge the support of NSF GFRP grant number DGE1144152 and the Research Foundation Flanders grant number 12O9115N. All fabrication was done in the Harvard Center for Nanoscale Sciences (CNS) clean room facility. We kindly thank the groups of Evelyn Hu and David Weitz at Harvard University for shared equipment and lab access.

* Email: capasso@seas.harvard.edu

[1] K. Wang, E. Schonbrun, P. Steinvurzel, and K. B. Crozier, Nature communications **2**, 469 (2011), ISSN 2041-1723, URL http://dx.doi.org/10.1038/ncomms1480.

[2] M. Righini, G. Volpe, C. Girard, D. Petrov, and R. Quidant, Physical Review Letters **100**, 8 (2008), ISSN 00319007.

[3] C. Min, Z. Shen, J. Shen, Y. Zhang, H. Fang, G. Yuan, L. Du, S. Zhu, T. Lei, and X. Yuan, Nature communications **4**, 2891 (2013), ISSN 2041-1723, URL http://www.pubmedcentral.nih.gov/articlerender.fcgi?artid=3863898{&}tool=pmcentrez{&}rendertype=abstract.

[4] K. Wang, E. Schonbrun, and K. B. Crozier, Nano Letters **9**, 2623 (2009), ISSN 15306984.

[5] A. Grigorenko, N. Roberts, M. Dickinson, and Y. Zhang, Nature Photonics **2**, 365 (2008).

[6] M. L. Povinelli, M. Lončar, M. Ibanescu, E. J. Smythe, S. G. Johnson, F. Capasso, and J. D. Joannopoulos, Optics letters **30**, 3042 (2005).

[7] G. Volpe, R. Quidant, G. Badenes, and D. Petrov, Physical Review Letters **96**, 238101 (2006), ISSN 0031-9007, URL http://link.aps.org/doi/10.1103/PhysRevLett.96.238101.

[8] D. Woolf, M. a. Kats, and F. Capasso, Optics letters **39**, 517 (2014), ISSN 1539-4794, URL http://www.ncbi.nlm.nih.gov/pubmed/24487854.

[9] K. Y. Bliokh, A. Y. Bekshaev, and F. Nori, Nature Communications **5**, 14 (2013), ISSN 2041-1723, 1308.0547, URL http://www.ncbi.nlm.nih.gov/pubmed/24598730$\delimiter"026E30F$nhttp://arxiv.org/abs/1308.0547.

[10] S. B. Wang and C. T. Chan, Nature Communications **5**, 1 (2014), ISSN 2041-1723, URL http://www.nature.com/doifinder/10.1038/ncomms4307.

[11] F. J. Rodríguez-Fortuño, N. Engheta, A. Martínez, and A. V. Zayats, Nature communications **6** (2015).

[12] A. Hayat, J. P. B. Mueller, and F. Capasso, Proceedings of the National Academy of Sciences **2015**, 201516704 (2015), ISSN 0027-8424, URL http://www.pnas.org/lookup/doi/10.1073/pnas.1516704112.

[13] D. G. Grier, Nature **424**, 810 (2003), ISSN 1476-4687, URL http://www.ncbi.nlm.nih.gov/pubmed/12917694.

[14] K. C. Neuman and S. M. Block, Review of scientific instruments **75**, 2787 (2004).

[15] D. C. Prieve, S. G. Bike, and N. A. Frej, Faraday Discussions of the Chemical Society **90**, 209 (1990).

[16] E.-L. Florin, A. Pralle, J. H. Hörber, and E. H. Stelzer, Journal of Structural Biology **119**, 202 (1997).

[17] A. A. Geraci, S. B. Papp, and J. Kitching, Physical review letters **105**, 101101 (2010).

[18] L. Liu, S. Kheifets, V. Ginis, and F. Capasso, Physical Review Letters **116**, 228001 (2016), ISSN 0031-9007, URL http://journals.aps.org/prl/abstract/10.1103/PhysRevLett.116.228001.

[19] J. Leach, H. Mushfique, R. di Leonardo, M. Padgett, and J. Cooper, Lab on a chip **6**, 735 (2006), ISSN 1473-0197, URL http://pubs.rsc.org/en/content/articlelanding/2006/lc/b601886f$\delimiter"026E30F$nhttp://pubs.rsc.org/en/content/articlelanding/2006/lc/b601886f{#}!divAbstract.

[20] A. Terray, J. Oakey, and D. W. M. Marr, Science **296**, 1841 (2002), ISSN 00368075.

[21] M. MacDonald, G. Spalding, and K. Dholakia, Nature **426**, 421 (2003).

[22] C. Lutz, M. Kollmann, and C. Bechinger, Physical review letters **93**, 026001 (2004).

[23] V. Garcés-Chávez, R. Quidant, P. Reece, G. Badenes, L. Torner, and K. Dholakia, Physical Review B **73**, 085417 (2006).

[24] A. Jonáš, P. Zemánek, and E.-L. Florin, Optics letters **26**, 1466 (2001).

[25] Y. Roichman, B. Sun, A. Stolarski, and D. G. Grier, Physical Review Letters **101**, 1 (2008), ISSN 00319007, 0806.4632.

[26] S. Wang and C. T. Chan, Optics express **24**, 2235 (2016).

[27] M. M. Salary and H. Mosallaei, Physical Review B **24**, 2235 (2016).

[28] A. Y. Bekshaev, K. Y. Bliokh, and F. Nori, Optics express **21**, 7082 (2013).

[29] Y. Yang, W.-P. Zang, Z.-Y. Zhao, and J.-G. Tian, Optics express **20**, 25681 (2012).

[30] C. Lóxpez-Mariscal, J. C. Gutiérrez-Vega, G. Milne, and K. Dholakia, Optics express **14**, 4182 (2006).

[31] K. Volke-Sepulveda, V. Garcés-Chávez, S. Chávez-Cerda, J. Arlt, and K. Dholakia, Journal of Optics B: Quantum and Semiclassical Optics **4**, S82 (2002).

[32] G. E. Uhlenbeck and L. S. Ornstein, Phys. Rev. **36**, 823 (1930), URL http://link.aps.org/doi/10.1103/PhysRev.36.823.

[33] K. Berg-Sørensen and H. Flyvbjerg, Review of Scientific Instruments **75**, 594 (2004), ISSN 00346748.

[34] T. A. Nieminen, N. du Preez-Wilkinson, A. B. Stilgoe, V. L. Loke, A. A. Bui, and H. Rubinsztein-Dunlop, Journal of Quantitative Spectroscopy and Radiative Transfer **146**, 59 (2014).

[35] See Supplemental Material at http://link... for a detailed discussion of the experimental setup, the measurement algorithms, the Mie theory calculations, and the data analysis.

[36] H. Brenner, Chemical Engineering Science **16**, 242 (1961).

[37] A. Goldman, R. G. Cox, and H. Brenner, Chemical Engineering Science **22**, 637 (1967).

[38] G. Nägele, Physics Reports **272**, 215 (1996).

[39] E. Almaas and I. Brevik, Journal of the Optical Society of America B **12**, 2429 (1995).

[40] R. Huang, I. Chavez, K. M. Taute, B. Lukić, S. Jeney, M. G. Raizen, and E.-L. Florin, Nature Physics **7**, 576 (2011).

[41] S. Kheifets, A. Simha, K. Melin, T. Li, and M. G. Raizen, science **343**, 1493 (2014).

[42] L. Liu, A. Woolf, A. W. Rodriguez, and F. Capasso, Proceedings of the National Academy of Sciences **111**, E5609 (2014), ISSN 0027-8424, URL http://www.pnas.org/lookup/doi/10.1073/pnas.1422178112.

[43] D. C. Prieve and J. Y. Walz, Applied optics **32**, 1629 (1993).